

Thermal diffusion in the IGM of clusters of galaxies

P. Shtykovskiy^{1,2} * and M. Gilfanov^{2,1*}

¹*Space Research Institute, Russian Academy of Sciences, Profsoyuznaya 84/32, 117997 Moscow, Russia*

²*Max-Planck-Institute für Astrophysik, Karl-Schwarzschild-Str. 1, D-85740 Garching bei München, Germany*

Accepted. Received; in original form

ABSTRACT

We revisit the phenomenon of elements diffusion in the intergalactic medium (IGM) in clusters of galaxies. The diffusion is driven by gravity, concentration and temperature gradients. The latter cause thermal diffusion, which has been so far ignored in IGM studies. We consider the full problem based on the Burgers' equations and demonstrate that the temperature gradients present in clusters of galaxies may successfully compete with gravity, evacuating metals from cooler regions. Under the combined action of gravity and temperature gradients, complicated metallicity profiles with several peaks and depressions may be formed. For a typical cool core cluster, the thermal diffusion may significantly reduce and even reverse the gravitational sedimentation of metals, resulting in the depression in their abundance in the core. This may have implications for diagnostics of the low temperature plasma in the centers of clusters of galaxies.

Key words: X-rays: galaxy clusters.

1 INTRODUCTION

Clusters of galaxies are the largest gravitationally-bound objects in the Universe with thousands of galaxies residing in a dark matter-dominated potential. Hot intergalactic medium (IGM), constituting the majority of the baryonic matter in galaxy clusters, is a natural laboratory for plasma physics displaying a wide range of phenomena. Despite seemingly simple nature of galaxy clusters, understanding of physical processes in hot plasma of IGM is far from being complete.

Of particular importance is the heavy elements distribution. Indeed, on the one hand it affects significantly the outcome of cosmological measurements via the mean molecular weight and thus the derived mass of the clusters (e.g. Qin & Wu 2000; Chuzhoy & Nusser 2003) and the baryonic density (e.g. Ettori & Fabian 2006). On the other hand the X-ray spectrum of gas at low temperatures, $T \lesssim 3 \times 10^7$ K, is dominated by the emission lines, most important of which are associated with iron. The diagnostics of low temperature plasma in clusters of galaxies is based primarily on line emission from heavy elements and the distribution of the latter may have direct implications for various phenomena, including the cooling flow problem (Fabian 1994).

Despite the importance of the heavy element distribution, flat metallicity profiles are often assumed. This assumption may turn out to be too crude in some cases. Indeed, the starting point for the metallicity profile is the primordial abundance. It is, however, quickly modified by a number of competing processes such as metals injection by

supernovae, mixing and diffusion. Although the effects of the latter process are rather controversial and its relevance to IGM in clusters of galaxies is still under debate, the scenario where the diffusion plays a significant role in forming the metallicity profile does not seem to be entirely unrealistic.

The diffusion of heavy elements in the intracluster medium has been considered by e.g. Fabian & Pringle (1977); Gilfanov & Syunyaev (1984); Chuzhoy & Nusser (2003). Most studies focused on the gravitational separation (gravitational sedimentation) and found that it may result in significant changes of the gas composition throughout the cluster. Given the presence of temperature gradients in IGM, an additional type of diffusion may play a role, namely thermal diffusion. Although the importance of the latter in physics in general and in stellar physics in particular has been appreciated long ago (e.g. Thoul, Bahcall & Loeb 1994), it was largely ignored in the case of ISM in galaxies and IGM in cluster of galaxies. The exceptions are studies by Chuzhoy & Loeb (2004) who solved the full problem, however considered the case of isothermal cluster and Peng & Nagai (2008) who mentioned the potential relevance of the thermal diffusion effects in galaxy clusters. At first glance, simplified approach ignoring thermal diffusion may seem to be reasonable since the temperature variations in galaxy clusters are rather small. It turns out, however, that even moderate temperature gradient may be sufficient to compete the gravitational force. The consideration of the full problem including the effects of thermal diffusion is the subject of present paper.

The paper is structured as follows. In section 2 we dis-

* E-mail: pavel@iki.rssi.ru; gilfanov@mpa-garching.mpg.de

cuss the nature of the metallicity profiles in galaxy clusters. In section 3 we describe the basic equations, numerical scheme and simulate the diffusion-driven evolution of a model galaxy cluster. Finally, in section 5 we discuss the obtained results.

2 METALLICITY PROFILES IN GALAXY CLUSTERS

Although the observed metallicity profiles are known to vary from cluster to cluster, they do exhibit some similarities in their behaviour (e.g. Vikhlinin et al. 2005; Sanderson, O’Sullivan & Ponman 2009). Typically, in cool core (CC) clusters the heavy element abundance rises from the cluster outskirts to the core. At the same time in the central parts, $r \lesssim 10 - 20$ kpc, a fraction of CC clusters show a depression in metallicity, whose nature and even reality is still under debate (e.g. Werner et al. 2009).

The metallicity profiles in galaxy clusters form as a result of interplay between different processes such as injection of metals from the supernovae-driven galactic winds, turbulent mixing and diffusion. The importance of the latter in plasma with turbulent magnetic field has been debated for a long time (e.g. Bakunin 2005; Lazarian 2007). As it is well known, a magnetic field hinders the diffusion across the field lines. However, given the chaotic character of the field in a turbulent medium, the efficiency of transport processes may be high enough to make the diffusion and thermal conduction important (Narayan & Medvedev 2001). In the following we assume that this is indeed the case.

The diffusion is driven by the gravity, temperature and concentration gradients. Below we consider each in details.

(i) *Gravitational sedimentation.* The equilibrium distribution of heavy elements, $n_s \propto e^{-m_s g h / k T}$, is more concentrated towards the cluster’s center than that of the hydrogen. Thus, due to the gravitational force, heavy elements tend to sink towards the cluster center, while light elements rise.

(ii) *Thermal diffusion.* Thermal diffusion was discovered theoretically by Enskog and Chapman in the 1911-1917 (e.g. Chapman & Cowling 1952). A clear physical explanation of the effect has been given significantly later by Monchick & Mason (1967), who demonstrated that thermal diffusion results from the dependence of collisional frequency on the velocity of particles. In the gas composed of two elements, the effect of thermal diffusion is to evacuate the more massive and more highly charged species from the colder region of the gas. In the case of a gas with three species – the abundant light ions, electrons and a small admixture of heavy ions with charge Z_s and atomic masses A_s , the equilibrium distribution of the heavy element may be obtained analytically (Burgers 1969):

$$n_s(r) \propto T^{\alpha Z_s^2} \exp \left[-\frac{(A_s - 0.5 Z_s) m_p}{k_B} \int \frac{g(r)}{T(r)} dr \right], \quad (1)$$

where alpha is constant of the order of 3. This formula demonstrates the importance of thermal diffusion for heavy elements. Indeed, substituting $Z_S=26$ for the iron, we obtain $\gtrsim 2000$ for the power of T in the first multiplier. In practice,

however, the time required to reach the equilibrium distribution may easily exceed the Hubble time and such a steep abundance profile is not formed.

(iii) *Concentration gradients.* The diffusion driven by concentration gradients works to restore the uniform abundance profile.

Another process affecting the heavy elements distribution is turbulent mixing which tends to wash out the metallicity gradients. The effects of mixing depend on the spatial scales over which the turbulence is operating and on the chaotic velocities spectrum. Mixing may also be driven by dynamical effects such as “sloshing” (Ascasibar & Markevitch 2006).

In the next section we construct a model cluster of galaxies and calculate the evolution of its metallicity profile due to diffusion of elements. Our goal is to consider the full problem of diffusion for an idealized cluster in order to demonstrate the effects of heavy elements transport in galaxy clusters, with particular emphasis on the modifications brought about by the thermal diffusion. Construction of a fully self-consistent model is beyond the scope of this paper, therefore we make several simplifying assumptions, namely:

(i) We consider the idealized case of a static cluster assuming that it’s mass remains constant throughout the duration of simulations. In real case the cluster mass continuously grows via mergers and accretion of DM halos (e.g. Cohn & White 2005). Since we are mostly interested in cool core clusters which are (most likely) not affected significantly by mergers in the past few Gyrs (e.g. Santos et al. 2008; Poole et al. 2008), this should not compromise our results significantly.

(ii) We assume that there is an exact balance between heating and cooling of IGM which maintains the temperature profile constant throughout the simulations. This implies that the IGM heating via the thermal conduction (which accompanies diffusion as these are the two sides of one phenomenon) and due to action of the central AGN equal the radiative cooling. As shown by Guo, Oh & Ruszkowski (2008), a stable configuration of this kind may indeed exist.

(iii) The IGM enrichment due to the continuous injection of metals from galaxies is ignored.

(iv) The effect of mixing on the metallicity profile of the cluster is ignored.

The possible effect of the latter two processes is discussed in the section 4.5.

3 NUMERICAL EXPERIMENT

We consider a spherically-symmetric cluster of galaxies with multicomponent plasma residing in a dark matter dominated gravitational potential. The latter is assumed to follow the NFW profile (Navarro, Frank & White 1997). The cluster is assumed to be initially in the hydrostatic equilibrium.

3.1 Basic equations

We consider M species ($M - 1$ ions plus electrons) with concentrations n_s , mean velocities u_s , atomic masses A_s and charges Z_s . All species have the same temperature $T_s \equiv T$. The diffusion velocities w_s are defined as:

$$w_s \equiv u_s - u, \quad (2)$$

where u is the mean fluid velocity:

$$u = \frac{\sum_s n_s m_s u_s}{\sum_s n_s m_s}. \quad (3)$$

The hydrodynamics of multicomponent gases is governed by Burgers' equations (Burgers 1969). The Burgers' equations for the gas in the hydrostatic equilibrium (the mass, momentum and energy conservation equations) are (Burgers 1969; Thoul, Bahcall & Loeb 1994):

$$\frac{\partial n_s}{\partial t} + \frac{1}{r^2} \frac{\partial}{\partial r} [r^2 n_s (w_s + u)] = 0, \quad (4)$$

$$\frac{d(n_s k_B T)}{dr} + n_s m_s g - n_s Z_s e E = \sum_{t \neq s} K_{st} [(w_t - w_s) + 0.6(x_{st} r_s - y_{st} r_t)], \quad (5)$$

and

$$\frac{5}{2} n_s k_B \frac{dT}{dr} = \sum_{t \neq s} K_{st} \left\{ \frac{3}{2} x_{st} (w_s - w_t) - \right. \quad (6)$$

$$\left. - y_{st} [1.6 x_{st} (r_s + r_t) + Y_{st} r_s - 4.3 x_{st} r_t] \right\} - 0.8 K_{ss} r_s.$$

Here $g = [GM(r)/r^2]$ is the gravitational acceleration *modulus*, E is the radial electric field, $x_{st} = \mu_{st}/m_s$, $y_{st} = \mu_{st}/m_t$ with $\mu_{st} = m_s m_t / (m_s + m_t)$ and $Y_{st} = 3y_{st} + 1.3x_{st} m_t / m_s$. Coefficients in equations correspond to pure Coulomb potential with a long-range cutoff at the Debye length (Thoul, Bahcall & Loeb 1994). The quantities r_s are the so-called residual heat flow vectors introduced by Burgers (1969), playing the role of additional independent variables. The thermal diffusion arises due to the interference of equation 5 and the energy equation 6 via the r_s .

The friction coefficient between species s and t is:

$$K_{st} = (2/3) \mu_{st} (2k_B T / \mu_{st})^{1/2} n_s n_t \sigma_{st}, \quad (7)$$

where the cross section between particles s and t is:

$$\sigma_{st} = 2\sqrt{\pi} e^4 Z_s^2 Z_t^2 (k_B T)^{-2} \ln \Lambda_{st}. \quad (8)$$

We assume the Coulomb logarithm to be $\ln \Lambda_{st} = 40$ everywhere.

In addition, charge neutrality and the absence of currents should be satisfied throughout the plasma. The former is not imposed explicitly in our code and is used to control the solution, while the latter is used to close the system of Burgers' equations (see below).

3.2 Simulations

The galaxy cluster is assumed to be initially in the hydrostatic equilibrium, i.e. there is no net mass flow, $u = 0$. However, once diffusion starts to operate, the total pressure changes and the gas is pushed out of the equilibrium, $\nabla p + \rho g \neq 0$. Indeed, while heavy elements flow to the center of the cluster, hydrogen flows outwards and there is a net

outflow of particles. The gas adjusts itself to the new equilibrium configuration via the contraction on the hydrodynamical timescale. Given the much smaller timescale of the latter as compared to the diffusion timescale, the departure from equilibrium will be small enough for the hydrostatic equilibrium form of Burgers' equations to be valid throughout the lifetime of a cluster (see also sec. 3.2.3).

In order to solve the problem we use the following numerical scheme:

(i) Based on the concentrations of elements n_s^{k-1} on $k-1$ th time step, solve Burgers' equations (5) and (6) for the diffusion velocities w_s^{k-1} .

(ii) Given the diffusion velocities w_s^{k-1} , the total mass flow velocity u^{k-1} and n_s^{k-1} , solve the continuity equation for the concentrations on the next time slice n_s^k .

(iii) Solve the Euler equation

$$\frac{du}{dt} = -\frac{\nabla p}{\rho} - g \quad (9)$$

for the velocity u^k , restoring the hydrodynamic equilibrium in a cluster, using u^{k-1} and n_s^{k-1} .

Below we discuss each step in detail.

3.2.1 Diffusion velocity calculation.

Burgers' equations (eqs 5 and 6) present a linear inverse problem of the form $A \times y = b$ on the diffusion velocities w_s , heat vectors of species r_s and electric field E . The diffusion is driven by the gradients ∇T , ∇n_s , $\nabla p(g(r))$, with all these quantities residing on the r.h.s. b . Given the M species we have $2M+1$ unknowns and thus need $2M+1$ independent equations. Burgers' equations give us only $2M-1$ independent equations, because diffusion velocities appear in eqs. 5 and 6 only in the form $(w_s - w_t)$. The two additional conditions needed to close the system of Burger's equations are defined as follows:

$$\sum \rho_i w_i = 0, \quad (10)$$

which follows from the definition of the diffusion velocity (eqs 2 and 3). Finally the absence of electric currents gives:

$$\sum Z_i n_i u_i = 0 \quad (11)$$

The resulting system of equations is solved for the w_s and r_s using the singular value decomposition (SVD) method (Press et al. 1992).

3.2.2 Continuity and Euler equations.

The problem we are solving is a mixed advection-diffusion problem. We have found that it can be solved with sufficient accuracy using the combination of forward-time centered-space (FTCS) and Lax methods (Toro 1999), with the former applied to the continuity equation and the latter to Euler equation. The Lax method is known to introduce numerical diffusion; however, we performed a number of tests and found that it is not crucial for our case (see Sec. 3.2.3).

We use a homogenous grid spanning from 0 to 2 Mpc with step $dr = 0.25$ kpc. The timestep is chosen to be small enough to ensure the stability of the scheme, $dt = 2 - 5 \cdot 10^{-5}$ Gyr.

Since we are mainly interested in the diffusion in the central region of the cluster, we are relatively free in the choice of the outer boundary condition. We assume that the galaxy cluster is immersed in the medium with constant density, i.e. there is an infinite reservoir of gas which maintains the gas density together with the element mass fractions at the outer boundary constant. In calculating velocities at the outer boundary we use one-sided derivatives.

At the inner boundary $r = 0$ the continuity equation has a singular point. Therefore we expand eq. (4) in the vicinity of zero and obtain the following expression for the concentration at the k -th time step:

$$n_{1,s}^k = n_{1,s}^{k-1} - 3 \times (dt/dr)n_{1,s}^{k-1}(u_2^{k-1} + w_{2,s}^{k-1}). \quad (12)$$

We also required that the density gradient should be equal to zero at $r = 0$ and used a one-sided derivative for the velocity gradient ∇u . In addition all velocities should be zero at the inner point: $w_s = 0$ and $u = 0$.

3.2.3 Code validation.

We further performed a number of tests to check the validity of our code.

(i) *Numerical diffusion.* We obtained the solution replacing the Lax method with the FTCS. The resulting code is free from numerical diffusion, however the FTCS-based scheme is less suited for our purpose due to a well-known instability of FTCS for hydrodynamical problems. On the other hand since the hydrodynamical terms in our equations appear only as a result of a slow diffusion process, we were able to obtain a stable solution for the 7 Gyr simulation. The solutions obtained using the combination of Lax+FTCS and FTCS+FTCS schemes are consistent with each other within a few percent.

(ii) *Boundary conditions.* We check that the solution is insensitive to the boundary conditions. For this purpose we run our code for 7 Gyr with different outer radii and found no significant difference. We also considered the opaque outer boundary, setting to zero all the velocities at the outer radius. The solution at $t = 7$ Gyr in this case is also consistent with the one for the default boundary conditions almost everywhere, within a fraction of a percent. Solutions obtained with different boundary conditions differ from each other only within ~ 100 kpc from the outer boundary. This dependence is unimportant and can be neglected.

(iii) *Hydrostatic equilibrium.* We also checked that the departures from the hydrostatic equilibrium are not too large, for the Burgers' equations to be valid, namely that $|\nabla p/\rho + g| \ll |\nabla p_s/\rho_s + g|$ throughout the duration of simulations. This condition is satisfied with an accuracy of better than a fraction of a percent.

(iv) *Electro-neutrality.* Since we do not use the electroneutrality condition explicitly in our code, we check that the final solution satisfies it. We obtain that $|\sum Z_i n_i/n_e - 1| \lesssim 10^{-5}$.

(v) *Comparison with an analytical solution.* In order to check the implementation of the Burgers' equations in the code, we consider a plasma composed of protons, electrons and a small admixture of iron in the hydrostatical equilibrium. Solving the Burgers' equations analytically we obtain the coefficient α in the power of temperature in eq. 1, $\alpha \approx$

3.1, and compute the equilibrium distribution of iron. For this distribution we calculate the diffusion velocities using our code and verify that they equal zero as expected for an equilibrium distribution. We obtain, that $w_{\text{Fe}} \ll 10^{-2}$ km/s.

4 RESULTS AND DISCUSSION

4.1 Model cluster

For the temperature profile of the cluster, $T(r)$, we use the analytical best-fit model for A262 from Vikhlinin et al. (2006). Outside the range of its applicability the profile was extended as illustrated in the Figure 1. The total mass density of the cluster is assumed to follow the NFW profile (Navarro, Frank & White 1997):

$$\rho_{NFW} = \frac{\rho_s}{(r/r_s)(1+r/r_s)^2}. \quad (13)$$

We take $r_s = 184$ kpc, the observed value for the A262 cluster (Vikhlinin et al. 2006).

Given the $T(r)$ and r_s and assuming hydrostatic equilibrium, we determine the value of ρ_s resulting in gas density $\rho_g(r)$ which follows as close as possible the analytical best-fit model for gas density from Vikhlinin et al. (2006). With the obtained value of normalisation, $\rho_s = 1.03 \times 10^{-25}$ g/cm³, the total mass inside the radius $r_x = 70$ kpc obtained integrating the $\rho_{NFW}(r)$ equals the total mass calculated using the temperature and gas density profiles (and their extrapolations) from Vikhlinin et al. (2006), assuming the hydrostatic equilibrium. The overall agreement between these two masses is better than $\approx 20 - 30\%$ in the range of 20–450 kpc with the limits reflecting the bounds of the region with a sufficient quality of data (Vikhlinin et al. 2006). The final gas density profile is calculated using the adjusted NFW profile $\rho_{NFW}(r)$, temperature profile $T(r)$ and assuming the hydrostatic equilibrium. The normalization of the gas density profile corresponds to a gas mass fraction within r_{500} (the radius where the overdensity is equal to 500) of $f_{500} = 0.14$. The resulting total mass, gas density and temperature profiles are shown in fig. 1.

To illustrate the role of the thermal diffusion, we also consider an isothermal cluster with temperature $kT = 2$ keV and the same total mass density profile. The initial gas density profile is calculated similarly to above, assuming the hydrostatic equilibrium (fig. 2).

We consider a 4-component plasma consisting of H^+ , He^{+2} , Fe^{+26} and electrons. The initial metallicity profiles are assumed to be flat with the mass fractions of hydrogen and iron being 0.75 and $1.8 \cdot 10^{-3}$ respectively. To demonstrate the effects of diffusion for different species, we also perform calculations replacing the Fe^{+26} by O^{+8} .

4.2 Diffusion in clusters of galaxies: temperature vs. gravity

We plot on fig. 1 and 2 the diffusion velocity profiles at the initial moment of time for a cool core and isothermal models respectively. Positive values correspond to outflow of particles, negative to inflow. As is clear from the plots, the presence of temperature gradients drastically changes the character of diffusion. While in an isothermal cluster the effect of diffusion is restricted to sedimentation of He and heavy

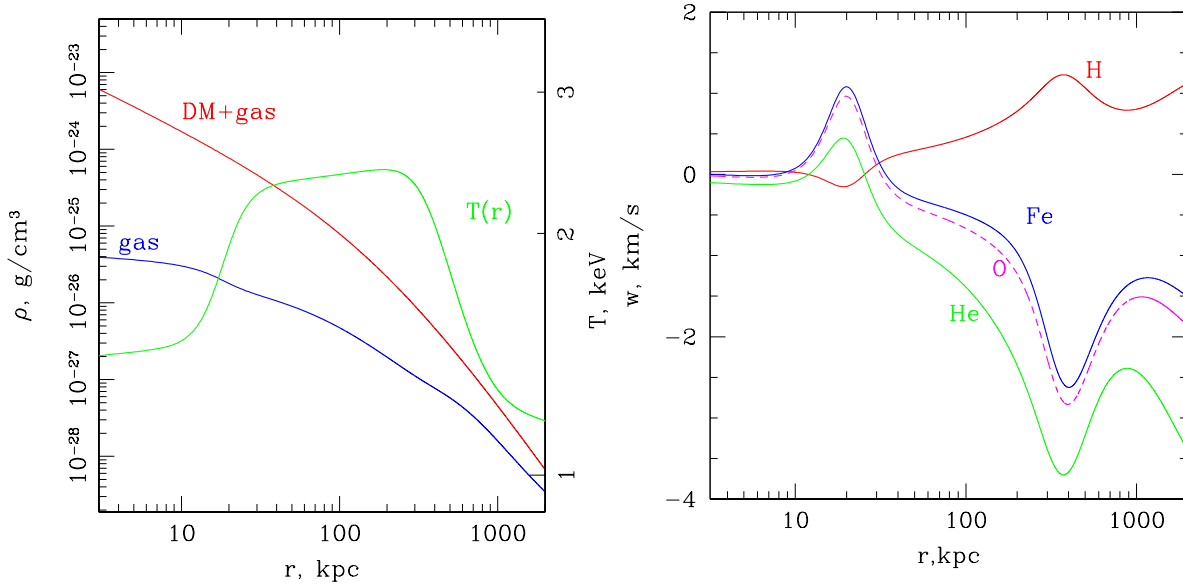


Figure 1. *Left:* Dark Matter and gas density profiles and temperature profile of the model galaxy cluster. *Right:* Corresponding initial diffusion velocity profiles for H (red), He (green), Fe (blue) and O (magenta, dashed line). Positive velocities correspond to outflow of particles, negative – to inflow. A positive peak at small radii and a negative one at the cluster outskirts are caused by the thermal diffusion and correspond to strong temperature gradients in the IGM (see the left panel).

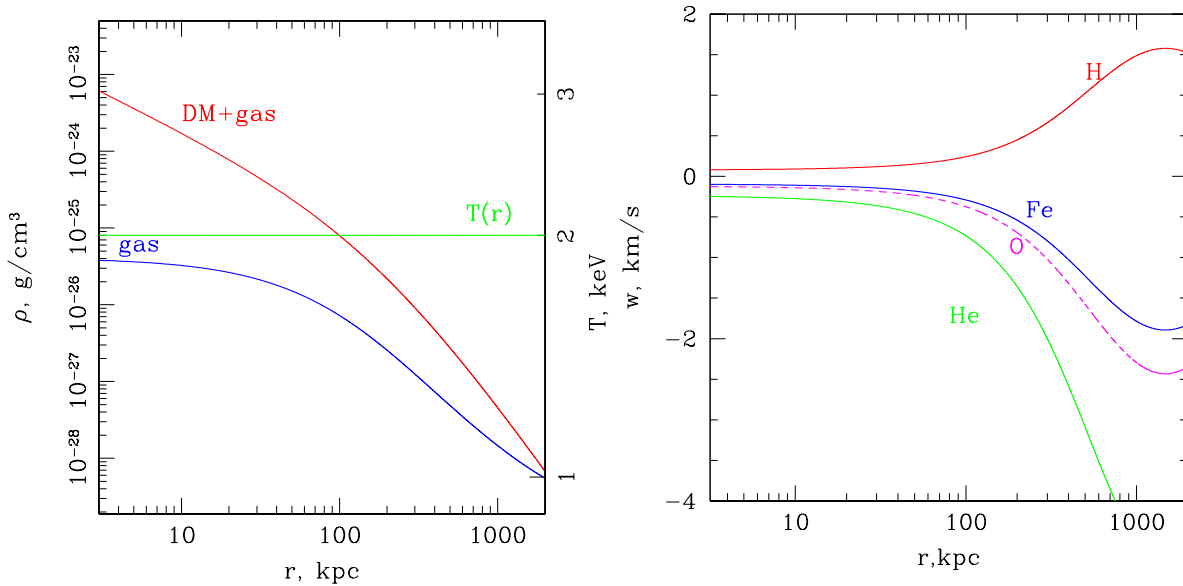


Figure 2. Same as in Fig.1 but for an isothermal cluster of galaxies.

nuclei, in the non-isothermal case the picture is more complicated. The combined effect of gravity and temperature gradients leads to formation of a complex diffusion velocity profile with prominent features at the positions of strong temperature gradients (~ 20 kpc and ~ 400 kpc in fig. 1). At small radii, the sharp decrease of temperature counteracts gravity and reverses the diffusion flow, evacuating heavy elements from the cool core of the cluster. On the other hand, the negative temperature gradient in the outer part of the cluster works in the same direction as the force of gravity, increasing the velocity of gravitational sedimentation. Note

that due to the lower temperatures and higher gas density, the diffusion velocities in the centers of cool core clusters are smaller than in higher temperature IGM usually considered in the context of the gravitational sedimentation of elements in clusters of galaxies (e.g. Chuzhoy & Nusser 2003). The goal of the present analysis is to study the possible role of thermal diffusion in the IGM. We therefore focused on the cool core clusters having strong temperature gradients, rather than on the high temperature clusters characterized by higher diffusion velocities. Because of the relatively small

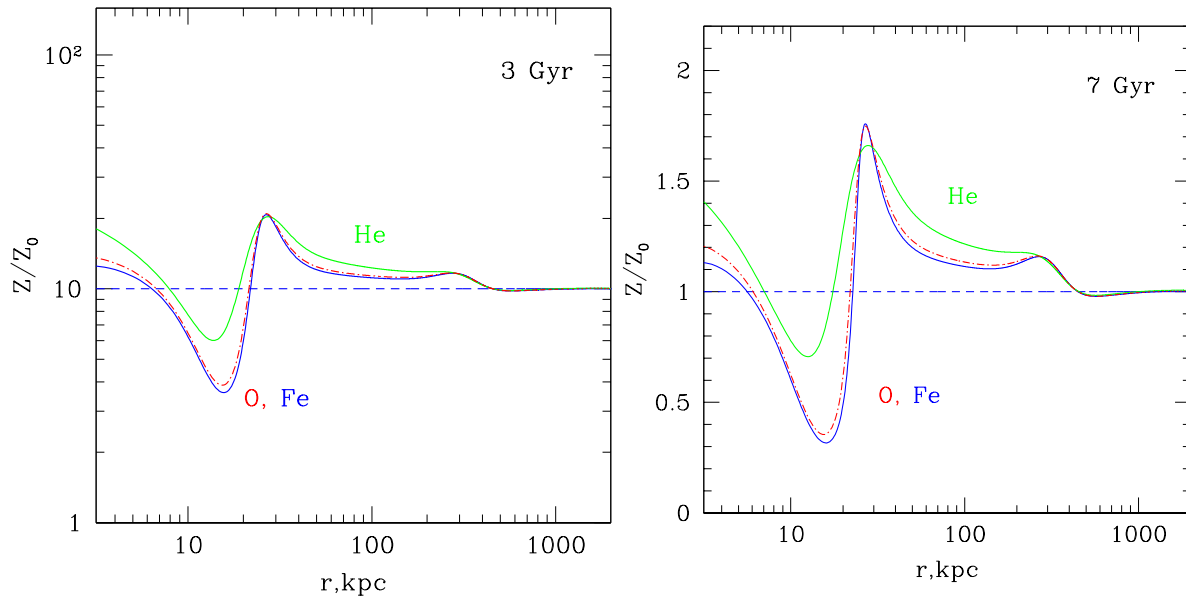


Figure 3. Abundance profiles for Fe (blue solid line), O (red dot-dashed line) and He (green line) in the model cluster of galaxies from Fig. 1 after 3 Gyr (left) and 7 Gyr (right).

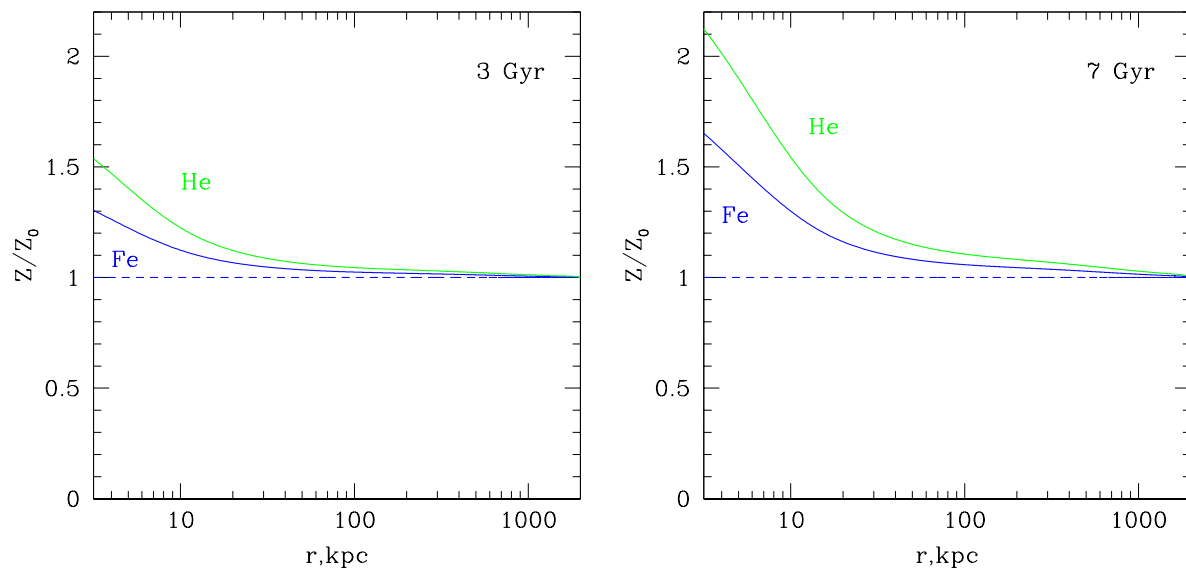


Figure 4. Same as in Fig. 3, but for an isothermal cluster from Fig. 2

diffusion velocity, ions can drift only through a small fraction of the cluster, $\lesssim 20$ kpc, during its lifetime.

The overall effect of diffusion is further illustrated by the metallicity profiles after 3 and 7 Gyrs shown in figure 3. At large radii the heavy elements flow inwards due to combined effect of thermal diffusion and gravity. The temperature peak at ~ 300 kpc leads to the enhancement of heavy elements abundance at this radius. At intermediate radii the temperature gradient is relatively weak and thus metals flow under the action of gravity to the center. Due to the strong temperature gradient at $r \sim 20$ kpc, the inward diffusion of heavy elements stops and the second peak is formed in heavy elements distribution. At the same time metals from

the core of the cluster flow up the temperature gradient, making the peak more prominent and creating a depression in the metallicity at smaller radii. Because of the nearly flat temperature distribution in the inner ~ 10 kpc, assumed here, the abundance at the center of the cluster is also somewhat enhanced by the gravitational sedimentation, with the effect being stronger for helium, than for iron. In contrast to this, the picture is much simpler in the isothermal cluster model shown in fig. 2. In this case the density profile evolution is driven by the gravitational sedimentation of heavy elements leading to a monotonic increase of their abundance towards the cluster center.

In figure 5 we compare the diffusion velocity profiles

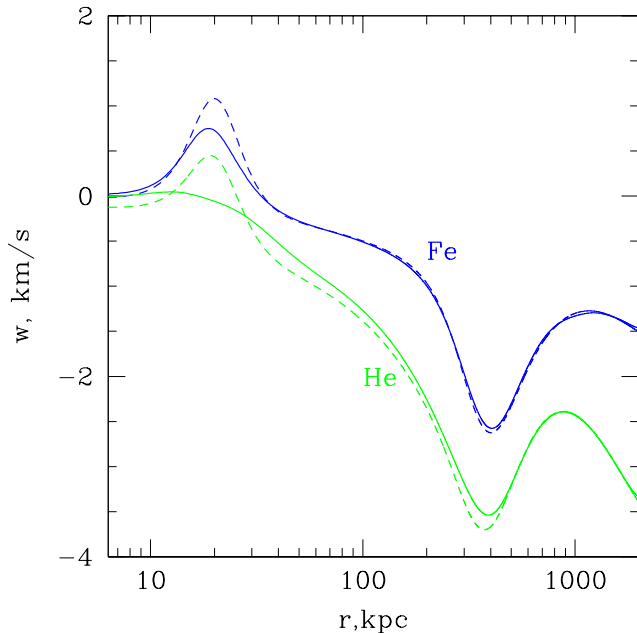


Figure 5. Diffusion velocity profiles for Fe (blue line) and He (green) in the model galaxy cluster after 7 Gyr. Dashed lines show the initial diffusion velocities.

after 7 Gyr with the initial distributions. Clearly, the outflow of Fe at small radii is only slightly reduced, while for He it almost disappears. The diffusion velocities outside the inner parts of the cluster remain almost unchanged.

4.3 Dependence on the atomic mass and charge

Both gravitational sedimentation and thermal diffusion velocities depend on the ion species. As is clear from Fig. 2, the gravitational sedimentation in an isothermal cluster is the most effective for the helium ions, with the higher Z ions such as Fe and O diffusing somewhat slower. At the same time, the diffusion velocities are almost equal for the latter two, $w_{Fe} \approx w_O$ (Chuzhoy & Nusser 2003). For a non-isothermal temperature profile, the equilibrium distribution of the heavy element depends on the element’s charge with more highly charged species being more concentrated towards peaks in temperature profile of the cluster (e.g. eq. 1). As a result, the abundance profile of He appears to be smoother than that of Fe (fig. 3). On the other hand, on the timescales of interest, the effect of diffusion for elements heavier than He is identical from the observational point of view. The strong charge dependence of thermal diffusion (eq. 1) becomes relevant only on significantly longer timescales, due to the small ∇T in the 30-200 kpc interval.

4.4 Dependence on the cluster parameters

The overall pattern of diffusion depends critically on the cluster parameters, due to the strong temperature, density and gravity dependence of diffusion velocities. Since the typical temperatures in clusters of galaxies vary from less than a 1 keV up to ~ 10 keV and the diffusion velocity scales with temperature as $w \propto T^{3/2}$ (e.g. Thoul, Bahcall & Loeb

1994), the variations in the diffusion velocity may exceed an order of magnitude. On the other hand, the temperature, gas density and gravity in clusters of galaxies are by no means independent (e.g. Vikhlinin et al. 2006). Thus the character of the diffusion is a result of the complex interplay between the cluster parameters.

The reversal of the diffusion flow for He and metals at small radii (fig. 1) is a consequence of a large gradient in the temperature profile, which counteracts the force of gravity. The balance between these two forces is sensitive to the details of the temperature distribution. Rather small and otherwise almost insignificant modifications of the temperature profile may lead to the diffusion pattern different from that shown in fig. 1 and 3. To illustrate this, we consider a cluster of galaxies with an (ad hoc) smoother temperature profile, characterized by smaller gradients in the cluster core, but with the same total mass distribution. The cluster parameters are shown in fig. 6. As is obvious from the figure, the initial distribution of the gas density does not differ significantly from our default model. However the diffusion velocity profile changes dramatically – the positive velocity peaks disappear for both elements and He velocity becomes negative in the entire range of radii (fig. 6). The resulting metallicity profile is correspondingly significantly smoother (cf. fig. 3). However, thermal diffusion counteracts the effect of the gravitational sedimentation in this case as well, significantly reducing its effect for He and resulting in a remarkable central depression in the Fe abundance.

Further decrease of the temperature gradient in the cluster core can make gravity the dominant factor. Based on the solution of Burgers’ equations we estimate that for the gravitational potential considered here, the thermal diffusion equals to the force of gravity for the temperature gradient of $\Delta T \sim 0.1$ keV per 20 kpc. Note that this is ~ 2 times smaller than the temperature gradient in the profile shown in the fig. 6, $\Delta T \sim 0.2$ keV per 20 kpc at $r = 20$ kpc.

4.5 Turbulent mixing and metals injection from cD galaxy

An idealized model constructed in this paper ignores turbulent mixing and metal enrichment of the IGM by the central cD galaxy - the two important factors which potentially may have a significant impact on the metallicity profiles. The turbulent mixing tends to smoothen the abundance distributions, while the cD galaxy increases the heavy element abundances in the inner parts of the cluster due to metals produced by (mostly) SNIa explosions. These two factors are discussed below.

In order to estimate role of the cD galaxy, we measure the K-band luminosity of A262 using the image from 2MASS Extended Source Image Server (<http://irsa.ipac.caltech.edu/applications/2MASS/PubGalPS/>) and based on the calibration of Mannucci et al. (2005) for E/S0 galaxies convert it to the SN Ia rate. Combining the latter with the iron yield of $\eta \sim 0.7 M_\odot$ (Iwamoto et al. 1999) and assuming perfect mixing of the SNIa ejecta with IGM, we obtain the iron injection rate of $8.0 \cdot 10^{-3} M_\odot/\text{yr}$ within the inner ≈ 19 kpc of the cluster. On the other hand, given the diffusion velocity, $w_{Fe} \approx 10^5$ cm/s, and concentration of iron at this radius (see fig. 1), we obtain the diffusion-driven iron outflow

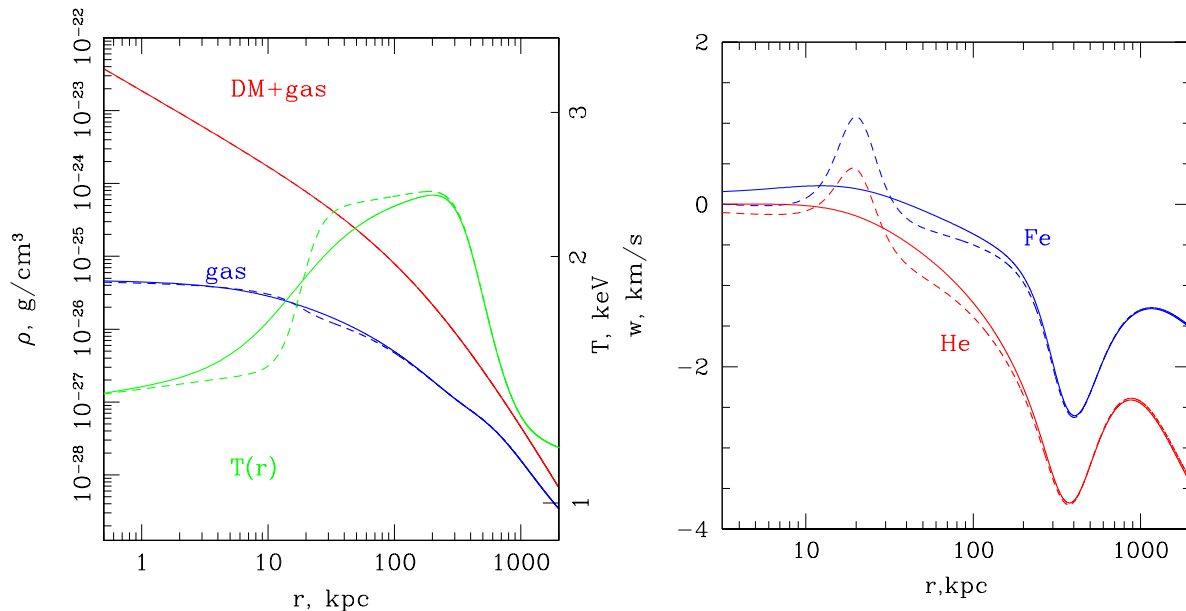


Figure 6. *Left:* Dark Matter, gas density and temperature profiles in the model galaxy clusters with an (ad hoc) temperature distribution with a moderate gradient in the core. The total mass distribution is the same as in our default model shown in fig. 1. *Right:* Diffusion velocity profiles for He (red) and Fe (blue) at the initial moment of time. For comparison, the dashed lines in both panels show profiles for the case of a large temperature gradient from fig.1. Unlike the latter case, He flows inwards over all radii.

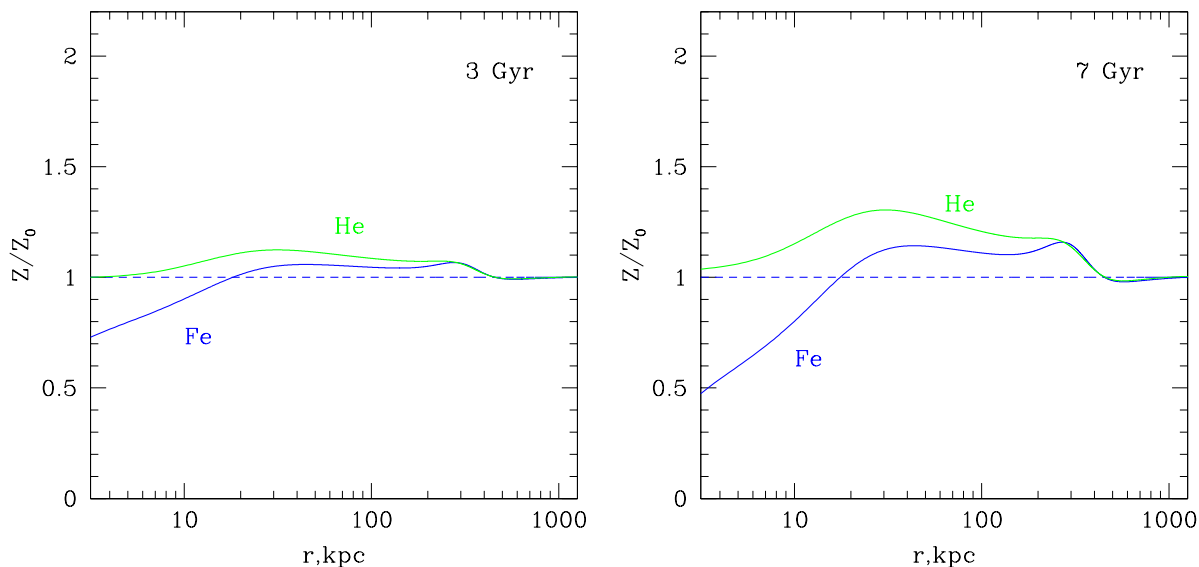


Figure 7. *Left:* Abundance profiles for Fe (blue solid line), and He (green line) in the model galaxy cluster from fig. 6 after 3 Gyr. *Right:* The same, but after 7 Gyr.

from the same region of $\approx 2.3 \cdot 10^{-3} M_{\odot}/\text{yr}$, which is several times smaller than the iron injection rate. The relation between the outflow and injection rates is opposite for α -elements. Indeed, assuming the oxygen yield of $\approx 0.1 M_{\odot}$ and solar metallicity, the oxygen injection rate is $\approx 1.1 \cdot 10^{-3} M_{\odot}/\text{yr}$, which is several times smaller than the outflow rate, $\approx 4.9 \cdot 10^{-2} M_{\odot}/\text{yr}$. Taking these numbers at the face value, we may conclude that the impact of the cD galaxy on metallicity profiles varies from significant for iron peak elements to negligible for α -elements.

We assumed above that complete mixing of the Supernova ejecta with IGM takes place. However, the details of the SN ejecta interaction with the ICM are poorly understood. Indeed, the assumption of the total mixing leads to unreasonably high iron abundance in the cluster core, as illustrated by the following calculation. Assuming that the iron injection rate in A262 follows the stellar mass profile and taking into account the metal injection by Supernovae via an additional source term in eq. 4, we repeated the calcu-

lation of the metallicity profile evolution described in sec. 3.¹ This resulted in a strongly peaked iron profile (Fig.8) with unrealistically high metallicity in the center of the cluster, $Z \approx 7 Z_{\odot}$ within the inner 10 kpc. Such a high iron abundance in the cluster core contradicts to observations of clusters of galaxies, in particular to the iron distribution in A262 measured by Vikhlinin et al. (2005), pointing at the need of a more sophisticated model. Similar results were obtained by Rebusco et al. (2006), who found the observed metallicity profiles in galaxy clusters to be broader than predicted under the assumption that the rate of metals injection follows stellar light distribution. A possible explanation of such a discrepancy is offered by the turbulent mixing driven by the central AGN activity. This requires turbulent diffusion coefficients of $6 \cdot 10^{27} - 5 \cdot 10^{29} \text{ cm}^2/\text{s}$, corresponding to mixing length scales of 1–35 kpc and gas velocities $\approx 200 - 400 \text{ km/s}$ (Rebusco et al. 2006). However, the role of this process in the particular case of A262 and other cool core clusters is unclear. Indeed, the presence of steep temperature and abundance gradients (Vikhlinin et al. 2005, 2006) rules out any significant mixing operating on spatial scales exceeding $\sim 10 \text{ kpc}$, thus excluding a large part of the parameters space required for the turbulent mixing interpretation.

To conclude, the role of mixing and metal enrichments remains to be controversial. An attempt to include them in the model in a straightforward manner leads to an apparent conflict with observations. This suggests that the role of these processes may be overestimated. Secondly, this points at the need of more sophisticated models. Consideration of such models will be a subject of the forthcoming paper.

5 CONCLUSIONS

We considered the effects of element diffusion in the intergalactic medium on the metallicity profiles in clusters of galaxies. The diffusion processes in the IGM are driven by the gravity, concentration and temperature gradients. Gravity forces metals to sink towards the center, concentration gradients act to restore the uniform distribution, and the temperature gradients tend to evacuate heavy elements from the low temperature regions in the IGM. So far, attention has been paid to gravitational sedimentation, while thermal diffusion has been largely excluded from consideration. We demonstrate that the latter may drastically change the pattern of the diffusion and thus may play a significant role in formation of the metallicity distribution in IGM.

We performed numerical simulations of the diffusion in the IGM of clusters of galaxies based on the full set of Burgers' equations. In order to illustrate the effect of thermal diffusion we considered three different models of cluster of galaxies with the same total mass profile but different temperature distributions: isothermal, and with large and moderate temperature gradient (figs. 1, 2, 6). The evolution of metallicity profiles are shown on figs. 3, 4 and 7. As illustrated by these plots, the combined effects of the temperature gradients and gravity may result in a rather complex metallicity profiles in clusters of galaxies.

¹ Note, that due to the limited coverage of A262 by 2MASS, the metal injection rate at $r \gtrsim 19 \text{ kpc}$ is somewhat underestimated. This, however, does not change our conclusions.

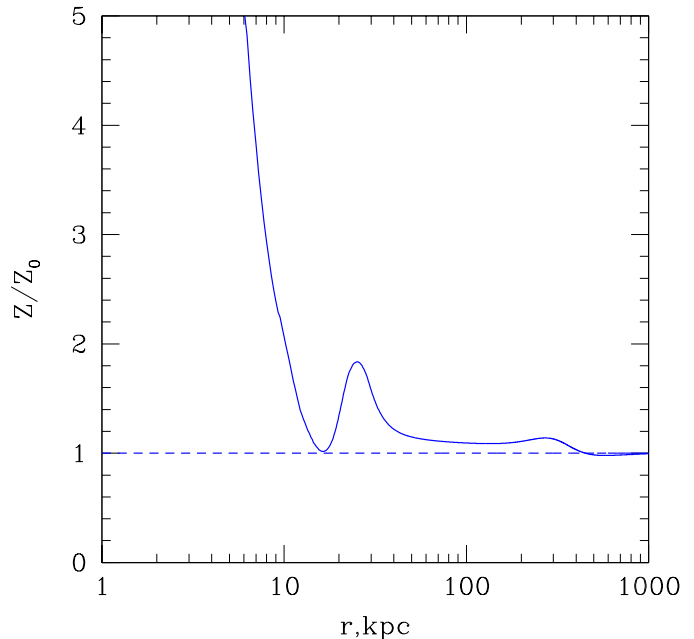


Figure 8. Abundance profile for Fe in the model galaxy cluster with injection of metals by cD galaxy after 7 Gyr. See section 4.5 for details.

The efficiency of transport processes in IGM is still under debate. However, if element diffusion does operate in clusters of galaxies, its overall effect on metallicity distributions may be opposite to what was previously thought, based on simplified considerations of isothermal IGM. Our results show that even moderate temperature gradients, $\sim 0.5 \text{ keV}$ per 100 kpc may be sufficient to counteract the force of gravity and to stop and even to reverse the diffusion flow of metals, thus preventing enhancement of heavy element abundances in the center due to gravitational sedimentation. It is especially relevant to the cool core clusters, where the thermal diffusion may lead to depletion of metals in the cluster core. The implications of this process for the diagnostics of the low temperature plasma in the centers of clusters of galaxies will be considered in the forthcoming paper (Shtykovskiy & Gilfanov, in preparation).

Acknowledgements. PS acknowledges support from the President of the Russian Federation grant NSh-5579.2008.2, the program of the Presidium of Russian Academy of Sciences (RAS) "The origin, structure and evolution of objects in the Universe" (P-07), and the program of RAS OFN-17. PS would like to thank Max-Planck-Institute for Astrophysics, where part of this work was done for their hospitality. We also would like to thank the anonymous referee for useful comments on the manuscript.

REFERENCES

- Ascasibar, Y., Markevitch, M., 2006, ApJ, 650, 102
- Bakunin, O., G., 2005, PPCF, 47, 1857
- Burgers, J., M., 1969, Flow Equations for Composite Gases. New York: Academic Press
- Chapman, S., Cowling, T., G., 1952, The Mathematical

- Theory of Non-uniform Gases. Cambridge, UK: Cambridge University Press
- Chuzhoy, L., Nusser, A., 2003, MNRAS, 342L, 5C
- Chuzhoy, L., Loeb, A., 2004, MNRAS, 349L, 13
- Cohn, J., D., White, M., 2005, APh, 24, 316
- Ettori, S., Fabian, A., C., 2006, MNRAS, 369L, 42
- Fabian, A., C., Pringle, J., E., 1977, MNRAS, 181P, 5
- Fabian, A., C., 1994, ARA&A, 32, 277
- Guo, F., Oh, S., P., Ruszkowski, M., 2008, ApJ, 688, 859
- Gilfanov, M., R., Syunyaev, R., A., 1984, SvAL, 10, 137
- Iwamoto, K., Brachwitz, F., Nomoto, K., Kishimoto, N., Umeda, H. et al., 1999, ApJS, 125, 439
- Lazarian, A., 2007, AIPC, 932, 58
- Mannucci, F., Della Valle, M., Panagia, N., Cappellaro, E., Cresci, G. et al., 2005, A&A, 433, 807
- Monchick, L., Mason, E., A., 1967, PhFl, 10, 1377
- Narayan, R., Medvedev, M., V., 2001, ApJ, 562L, 129
- Navarro, J., F., Frenk, C., S., White, S., D. M., 1997, ApJ, 490, 493
- Peng, F., Nagai, D., 2008, arXiv0808.3769P
- Poole, G., B., Babul, A., McCarthy, I., G., Sanderson, A. J. R., Fardal, M., 2008, MNRAS, 391, 1163
- Press, W., H., Teukolsky, S., A., Vetterling, W., T., Flannery, B., P., 1992, Numerical recipes in C. The art of scientific computing. Cambridge: University Press, 2nd ed.
- Qin, B., Wu, X.-P., 2000, ApJ, 529L, 1
- Rebusco, P., Churazov, E., Bhringer, H., Forman, W., 2006, MNRAS, 372, 1840
- Santos, J., S., Rosati, P., Tozzi, P., Boehringer, H., Ettori, S. et al., 2008, A&A, 483, 35
- Sanderson, A., O'Sullivan, E., Ponman, T., 2009, arXiv0902.1747
- Thoul, A., A., Bahcall, J., N., Loeb, A., 1994, ApJ, 421, 828
- Toro, E., F., 1999, Riemann Solvers and Numerical Methods for Fluid Dynamics. Berlin: Springer Verlag.
- Vikhlinin, A., Markevitch, M., Murray, S., S., Jones, C., Forman, W. et al., 2005, ApJ, 628, 655
- Vikhlinin, A., Kravtsov, A., Forman, W., Jones, C., Markevitch, M. et al., 2006, ApJ, 640, 691
- Werner, N., Zhuravleva, I., Churazov, E., Simionescu, A., Allen, S. W. et al., 2009, arXiv0904.0254